Available online at www.sciencedirect.com
ScienceDirect
Trans. Nonferrous Met. Soc. China 35(2025) 3134−3146
Transactions of Nonferrous Metals Society of China
www.tnmsc.cn

Effect of antimony and arsenic on gold enhancement capture during iron matte smelting of refractory gold concentrate by exclusion method

Bai-qi SUN[1], Wei-feng LIU[1,2], Du-chao ZHANG[1,2], Lin CHEN[1,2], Xu-heng LIU[1,2], Tian-zu YANG[1]

1. School of Metallurgy and Environment, Central South University, Changsha 410083, China;
2. National Engineering Research Center of Low-carbon Nonferrous Metallurgy, Central South University, Changsha 410083, China

Received 19 July 2024; accepted 3 March 2025

Abstract: Based on the properties of antimony (Sb) and arsenic (As), a method was proposed to enhance gold recovery during iron matte smelting. The impact of Sb and As on gold enhancement capture was investigated using an exclusion method. The results demonstrated that both Sb and As significantly improved the gold recovery rate. As the Sb or As content increased, the gold recovery rate increased. The enhancement effect of Sb was better than that of As, and the optimal results were achieved through the synergistic effects of Sb and As. Under optimized conditions, the gold recovery rate reached 97.12%, whereas the gold content in the slag decreased to 1.70 g/t. Sb captured and aggregated free gold as an Au−Sb alloy, whereas As−Fe alloy also captured free gold. The growth of the gold-captured phase size enhanced the settling velocity, thereby promoting gold recovery.

Key words: refractory gold concentrate; Au−Sb alloy; As−Fe alloy; enhancement effect; iron matte; capture gold

1 Introduction

With the rapid depletion of high-grade gold ore resources, refractory gold ores have become critical raw materials for the gold industry. Efficient recovery of gold while minimizing environmental pollution is a current research hotspot. Refractory gold ores are those in which the gold leaching rate is less than 85% when subjected to cyanidation. Owing to minerals encapsulation [1,2], interference from impurities [3,4], and "gold robbery" by adsorbents [5,6], the efficiency of gold extraction through direct cyanidation leaching is always low.

Currently, there are two primary methods for treating refractory gold ores: pretreatment−leaching and pyrometallurgical processes. The pretreatment of refractory ores is performed to break minerals inclusions and expose the gold. Commonly used pretreatment methods include oxidative roasting [7,8], oxidative leaching [9,10], and bio-oxidative leaching [11]. Following pretreatment, cyanide leaching [12,13], non-cyanide leaching [14−17], or bio-oxidation leaching [18−20] is conducted. The pyrometallurgical process involves the introduction of refractory gold ores into heavy-metal pyro-metallurgical systems to concentrate gold in metal sulfides or metals [21−23]. Subsequently, gold is recovered from the intermediate product. This method is also known as the refractory gold ore–heavy metal synergistic smelting process [24,25].

However, current gold extraction processes from refractory gold ores suffer from various shortcomings, such as environmental pollution risks, low gold leaching rates, and extended production periods. Consequently, there is an urgent need to develop clean and efficient technologies for extracting gold from refractory gold ores to ensure

Corresponding author: Wei-feng LIU, Tel: +86-13548654403, E-mail: liuweifeng@csu.edu.cn
https://doi.org/10.1016/S1003-6326(25)66871-3

the sustainable development of the gold industry.

The advantages of pyrometallurgical processes, including wide raw material adaptability and high gold recovery rates, render them suitable for extracting gold from refractory gold ores. YANG et al [26,27] proposed a novel method for extracting gold from refractory gold ores using iron matte smelting.

Antimony (Sb) and arsenic (As) are considered harmful impurities in gold ores. However, in mineralogy, these two elements are frequently associated with gold deposits. In copper smelting processes, Sb can affect the distribution behavior of precious metals [28,29]. Based on these characteristics, these traditionally harmful elements have been utilized to promote gold recovery.

In this study, the effects of Sb and As on gold enhancement capture during iron matte smelting from refractory gold concentrate were studied by exclusion method. The related mechanisms were also investigated. Initially, the effects of Sb and As on gold enhancement capture were investigated both qualitatively and quantitatively. Subsequently, the effects of Sb and As on the occurrence state of gold and the embedding relationships of typical minerals within the iron matte were studied. Finally, the core mechanism was elucidated. These findings indicate that Sb and As can significantly enhance gold capture, resulting in a rapid gold recovery process with a high recovery rate and efficiency.

2 Experimental

2.1 Material

The experimental raw material was an As- and Sb-bearing refractory gold concentrate provided by a company in Gansu, China. The mineral was dried at 50 °C and finely ground to a particle size <0.074 mm.

The primary chemical compositions of the As- and Sb-bearing refractory gold concentrate were as follows: iron (19.66 wt.%), sulfur (16.48 wt.%), silicon (14.50 wt.%), aluminum (4.37 wt.%), arsenic (6.17 wt.%), and antimony (4.07 wt.%). The contents of gold and silver were 36.20 and 38.40 g/t, respectively.

The phase composition was determined using X-ray diffraction (XRD), as shown in Fig. 1. The concentrate comprised pyrite (18.60 wt.%), arsenopyrite (7.67 wt.%), quartz (25.26 wt.%), and mica. Sb and As were present in the forms of stibnite (3.53%) and arsenopyrite, respectively.

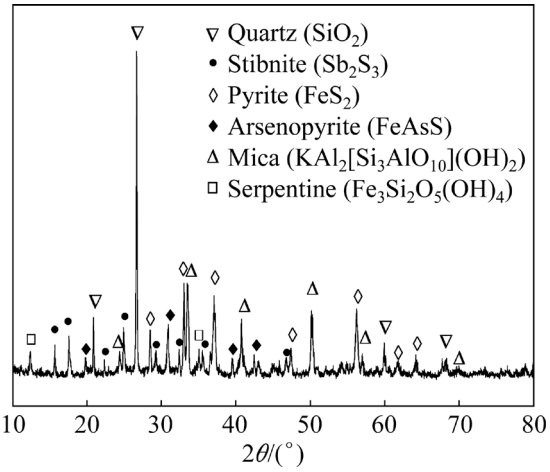

Fig. 1 XRD pattern of As- and Sb-bearing refractory gold concentrate

2.2 Research methodology

This study explored the effects of Sb and As on gold enhancement capture during iron matte smelting and the associated mechanisms. The research methodology is illustrated in Fig. 2.

Firstly, an exclusion method was employed to qualitatively investigate the impact of Sb and As on the gold capture process by iron matte. The gold recovery rates of the As- and Sb-bearing gold concentrate and the Sb-removed gold concentrate were compared to emphasize the effect of Sb on gold enhancement capture. Subsequently, the gold recovery rates of the Sb-removed gold concentrate were compared to those of the As-removed gold concentrate, highlighting the effect of As on gold enhancement capture.

Secondly, a quantitative study of the enhancement effects of Sb and As on gold capture was conducted. Sb and As were added in measured amounts to the As-removed gold concentrate for the experiments. Changes in the gold recovery rates and gold content in the slag were observed to confirm the impact of the Sb and As concentrations on gold recovery. Furthermore, Sb and As were added simultaneously to study their synergistic effects on gold enhancement capture.

Finally, the occurrence state of gold and the embedding relationships of typical mineral phases in the iron matte were researched to explore the enhancement.

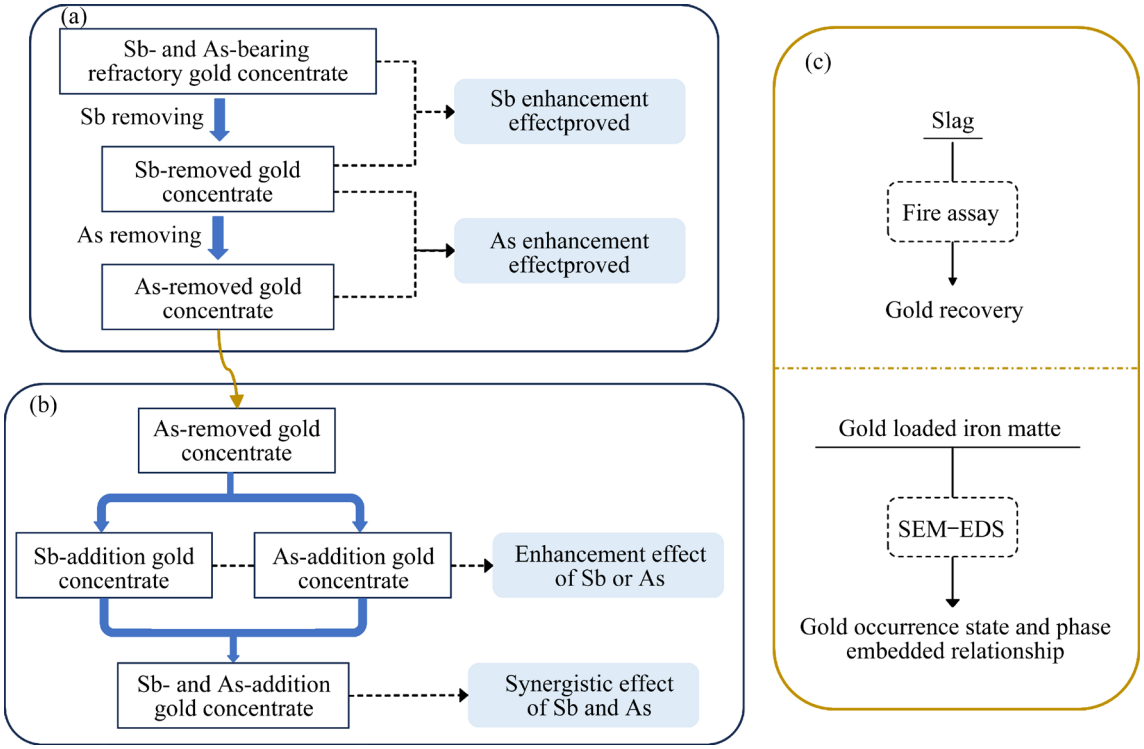

Fig. 2 Diagram of research methodology: (a) Qualitative research; (b) Quantitative research; (c) Detection and analysis

For ease of description, abbreviations for the raw materials are used in this paper, as presented in Table 1.

Table 1 Abbreviations for experimental raw materials

Raw material	Abbreviation
Arsenic- and antimony-bearing refractory gold concentrate	As- and Sb-bearing gold concentrate
Antimony-removed refractory gold concentrate	Sb-removed gold concentrate
Antimony- and arsenic-removed refractory gold concentrate	As-removed gold concentrate
Antimony(only)-addition refractory gold concentrate	Sb-addition gold concentrate
Arsenic(only)-addition refractory gold concentrate	As-addition gold concentrate
Antimony addition in arsenic-bearing refractory gold concentrate	Sb- and As-addition gold concentrate

2.3 Experimental procedure

The smelting experiment was conducted in a muffle furnace using a clay crucible as the container. Firstly, the raw materials and other agents were mixed and loaded into the clay crucible. Subsequently, the heating program of the muffle furnace was initiated. When the furnace temperature reached 900 °C, the crucible was placed inside the muffle furnace. When temperature reached 1200 °C, the reaction maintained for a period. Then, the crucible was taken out and allowed to cool naturally. Finally, the masses of the crucible, slag, and iron matte were recorded, and the slag and iron matte were preserved for further analysis.

The antimony removal experiment was conducted in a constant-temperature water bath under magnetic stirring. A beaker was used as the experimental container, and the leaching residue was the Sb-removed gold concentrate. Conversely, the arsenic removal experiment was conducted in a muffle furnace. The experimental container used for this process was a porcelain boat, and the roasted sand was the As-removed gold concentrate.

Both the smelting and leaching experiments were conducted in a fume hood with the emitted gases directed into a tail gas absorption tower for harmless treatment before discharge.

2.4 Detection and analysis

The gold contents of the raw materials and products were determined using the fire assay method.

XRD was used to determine the phase composition of the raw materials and products.

A TTRAX−3 XRD diffractometer (Rigaku Corporation, Japan) was used. The operating parameters were as follows: testing current of 300 mA, scanning speed of 10 (°)/min, and testing voltage of 50 kV.

Scanning electron microscopy (SEM) was used to determine the morphology of the products, and the chemical composition of the typical phases was determined using energy-dispersive X-ray spectroscopy (EDS). A scanning electron microscope (JEOL Ltd., Japan) equipped with an X-ray energy-dispersive spectrometer (model JSM−6360LV) was used. The magnification range was from 5 to 3×10^5 times, and the accelerating voltage changed from 0.5 to 30 kV.

Mineral liberation analysis (MLA) was employed to detect the phase contents of the raw materials and products as well as the distribution of elements. An MLA650 mineralogical automated analyzer (FEI Company, United States) was used. The XBSE-STD mode, with an acceleration voltage ranging from 200 V to 20 kV, and a magnification ranging from 500 to 10000 times, was adopted.

2.5 Data processing

The gold recovery rate was calculated by the following equation:

$$R_{\mathrm{A}}=\left(1-\frac{C_{\mathrm{A}}^{\mathrm{Slag}}M_{\mathrm{s}}}{C_{\mathrm{A}}M_{\mathrm{o}}}\right)\times100\% \tag{1}$$

where R_{A} represents the gold recovery rate (%); C_{A} and $C_{\mathrm{A}}^{\mathrm{Slag}}$ denote the gold contents of the raw material and slag (g/t), respectively; M_{o} and M_{s} represent the masses of the raw material and slag (g), respectively.

The increment of the gold recovery rate was calculated by

$$R_{\mathrm{R-Au}}=\frac{R_{\mathrm{A}}^{0}}{R'_{\mathrm{A}}}\times100\% \tag{2}$$

where $R_{\mathrm{R-Au}}$ represents the increment of the gold recovery rate; R_{A}^{0} represents the gold recovery rate when using the As-removed gold concentrate as the raw material for smelting; R'_{A} denotes the gold recovery rate of other smelting experiment.

The decrement of the gold content of the slag was calculated by

$$D_{\mathrm{C-Au}}=\left(1-\frac{C'_{\mathrm{A}}}{C_{\mathrm{A}}^{0}}\right)\times100\% \tag{3}$$

where $D_{\mathrm{C-Au}}$ represents the decrement of the gold content of the slag; C_{A}^{0} represents the gold content in the slag when using the As-removed gold concentrate as the raw material for smelting, and C'_{A} represents the gold content of the slag in other smelting experiment.

3 Results and discussion

3.1 Qualitative research on effects of Sb and As on gold enhancement capture

According to the research plan, it is essential to prepare Sb-removed gold concentrate and As-removed gold concentrate. The sodium sulfide leaching method was employed to remove Sb from the Sb- and As-bearing gold concentrate to prepare the Sb-removed gold concentrate. Subsequently, the roasting method was used to remove As from the Sb-removed gold concentrate, thereby producing the As-removed gold concentrate.

3.1.1 Sb and As removal experiment results

The conditions for the sodium sulfide leaching experiment were established as follows: a sodium sulfide addition coefficient of 1.2 (1.2 times the theoretical consumption of sodium sulfide according to Reaction (4)), sodium hydroxide concentration of 20 g/L, temperature of 60 °C, liquid/solid mass ratio (L/S) of 1.5, and reaction time of 2 h.

$$Sb_2S_3+3Na_2S=2Na_3SbS_3 \tag{4}$$

The conditions for the As-removal roasting experiment were: a temperature of 600 °C and a duration of 2 h. The Sb-removed concentrate and As-removed concentrate were obtained respectively.

Figure 3 shows the XRD patterns of the As- and Sb-bearing gold concentrate, Sb-removed gold concentrate, and As-removed gold concentrate. Table 2 presents the main chemical compositions of the Sb-removed gold concentrate and As-removed gold concentrate. As shown, after sodium sulfide leaching, the Sb content decreased to 0.03 wt.%, and the stibnite phase disappeared. Additionally, the As content in the roasted sand decreased to 0.18 wt.%, resulting in the disappearance of the arsenopyrite phase. Furthermore, during the roasting process, both pyrite and arsenopyrite were transformed into hematite and iron silicate, respectively. It was confirmed that the influences of Sb and As should be disregarded.

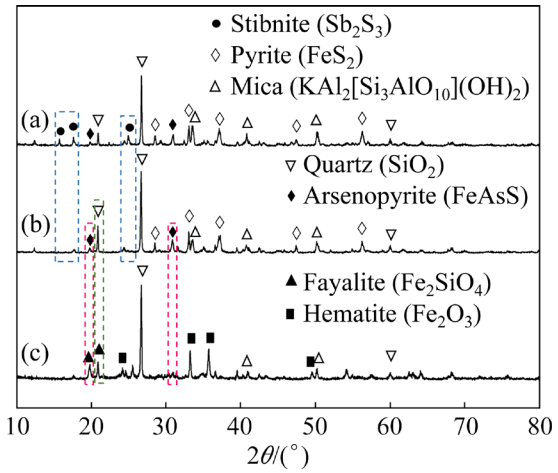

Fig. 3 XRD patterns of three raw materials: (a) As- and Sb-bearing gold concentrate; (b) Sb-removed gold concentrate; (c) As-removed gold concentrate

3.1.2 Iron matte smelting experiment results

Iron matte smelting experiments were conducted using the As- and Sb-bearing gold concentrate, Sb-removed gold concentrate, and As-removed gold concentrate as raw materials. The conditions were controlled as follows: m(FeO)/m(SiO_2)=1.2, m(CaO)/m(SiO_2)=0.4, temperature of 1200 °C, and duration time of 45 min.

According to Table 2, the sulfur content of the As-removed gold concentrate significantly decreased, which could severely affect iron matte smelting and the experimental results. To address this issue, specific proportions of the reducing agent and sulfur were added to the As-removed gold concentrate.

The results of the iron matte smelting process are listed in Table 3. The removal of Sb resulted in a noticeable decrease in the gold recovery rate, accompanied by a significant increase in the gold content of the slag. Furthermore, As removal led to an additional decline in the gold recovery rate. These results indicate that both Sb and As positively influenced the gold capture process. Notably, the effect of Sb on gold enhancement capture was significantly stronger than that of As. Therefore, Sb plays a crucial role in improving the efficiency of gold enhancement capture.

The microscopic morphologies and phase compositions of the iron mattes are shown in Fig. 4. As shown in Figs. 4(a), (b), and (c), the separation of Sb and As resulted in a significant reduction in the content of the alloy phases, such as SbAs, Sb, and FeAs, within the iron matte. Additionally, the number of high-contrast phases in the iron matte decreased. Concurrently, the gold recovery rate exhibited a gradual decline. It is suggested that alloy phases, such as SbAs, Sb, and FeAs, play a crucial role in gold enhancement capture by the iron matte.

The SEM and elemental surface screen images of the gold-loaded iron matte derived from the three raw materials are shown in Fig. 5. Sb and As not only affected the gold occurrence state, but also influenced the embedding relationships of the gold-bearing phases. In the presence of Sb and As in the iron matte, gold was found in the form of the Au−Sb alloy within metallic Sb, which was surrounded by the As−Fe alloy. When Sb was excluded, gold appeared in its elemental form and was encapsulated by the As−Fe alloy. Conversely, when As was excluded, gold existed as a free Au−Ag alloy within the iron matte. The main components of the gold-containing phases are listed in Table 4.

Table 2 Main chemical compositions of Sb-removed gold concentrate and As-removed gold concentrate (wt.%)

Raw material	Au	Ag	Fe	S	Sb	As	Al	Si	Ca
Sb-removed gold concentrate	40.18*	42.62*	21.82	18.29	0.03	5.74	4.85	16.10	1.94
As-removed gold concentrate	46.62*	51.85*	22.55	2.19	−	0.18	6.86	17.64	3.49

* g/t

Table 3 Iron matte smelting results from different raw materials

Raw material	Gold recovery rate/%	Gold content in slag/(g·t^{-1})
As- and Sb-bearing refractory gold concentrate	96.44	2.05
Sb-removed gold concentrate	85.67	10.85
As-removed gold concentrate	75.81	13.20

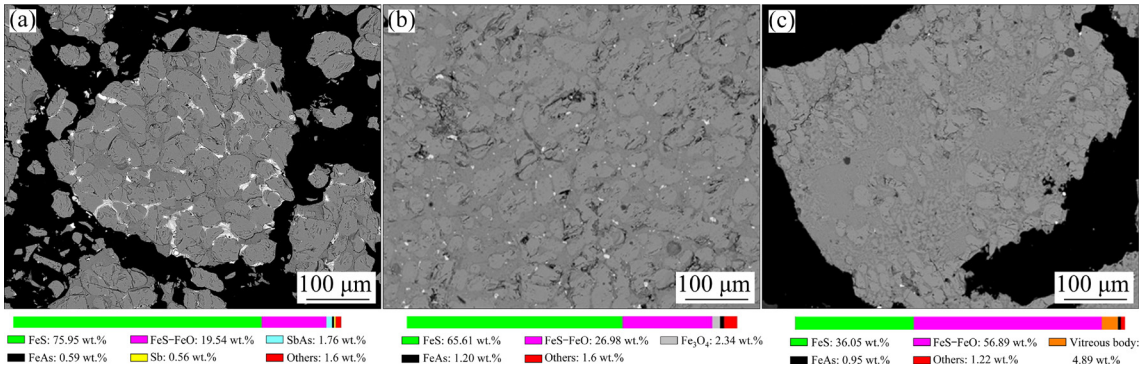

Fig. 4 SEM images and phase compositions of iron mattes from gold concentrates: (a) As- and Sb-bearing refractory gold concentrates; (b) Sb-removed gold concentrates; (c) As-removed gold concentrates

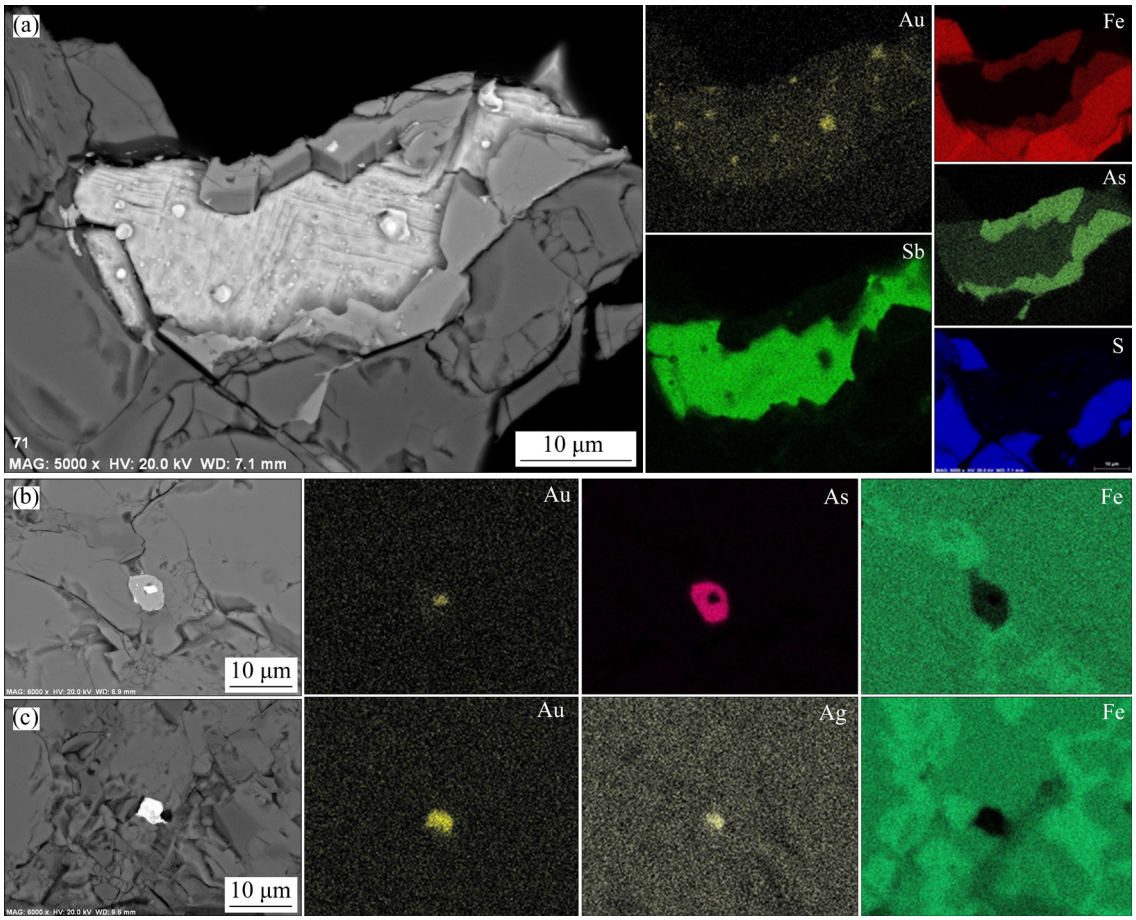

Fig. 5 SEM and elemental surface screening images of gold-containing iron matte from different concentrates: (a) As- and Sb-bearing gold concentrates; (b) Sb-removed gold concentrates; (c) As-removed gold concentrates

Table 4 Compositions of typical phases (wt.%)

Gold-contained phase	Au	Sb	Ag
Au−Sb alloy	50.97	49.03	−
Au−Ag alloy	50.20	−	49.80

Furthermore, the removal of Sb and As resulted in a progressive decrease in the particle size of the gold-containing phases. The settling behavior of the gold and gold-containing phases in the melt is theoretically based on Stokes' formula, which indicates that the settling velocity is related to the particle size. Sb and As influenced the settling behavior of the gold-containing phases, thereby changing the gold recovery rate.

In summary, both Sb and As can enhance the gold capture by iron matte. Sb demonstrated a more significant enhancement effect than As. The

exclusion method not only elucidated the effect of Sb and As on gold recovery, but also revealed the differences in their effectiveness.

3.2 Quantitative research on effect of Sb and As on gold enhancement capture

In this section, the effects of Sb and As contents in raw materials on the gold capture process were studied quantitatively, thereby examining the universality and controllability of the enhancement effect. In this study, Sb and As were quantitatively added into the As-removed gold concentrate, respectively.

3.2.1 Effect of Sb content

The experiments were conducted to study the effect of the Sb content in raw materials on the gold recovery rate and the gold content in slag. Antimony sulfide was used to modify the Sb content. The experimental conditions were as follows: $m(FeO)/m(SiO_2)$=1.2, $m(CaO)/m(SiO_2)$=0.4, temperature of 1200 °C, and duration time of 45 min. The results are presented in Fig. 6.

As the Sb content increased from 0 to 4 wt.%, the gold recovery rate increased from 75.81% to 94.80%, representing an increase proportion of 25.05%. Concurrently, the gold content in the slag decreased from 13.20 to 3.05 g/t, reflecting a decrease proportion of 76.89%. Moreover, when the Sb content increased, the increment rate in gold recovery rate gradually diminished. Sb significantly enhanced gold capture in iron matte with an optimal Sb content of 4 wt.%.

The elemental surface scanning images of the iron matte from the experiment with 4 wt.% Sb content are shown in Fig. 7. A significant amount of Au−Sb alloy was distributed within the metallic Sb, indicating that Sb altered the occurrence state of gold. In addition to gold, no other elements were found in Sb. A strong and exclusive tendency to form the Au−Sb alloy was observed. It is believed that the formation of the Au−Sb alloy was the main reason for the enhancement.

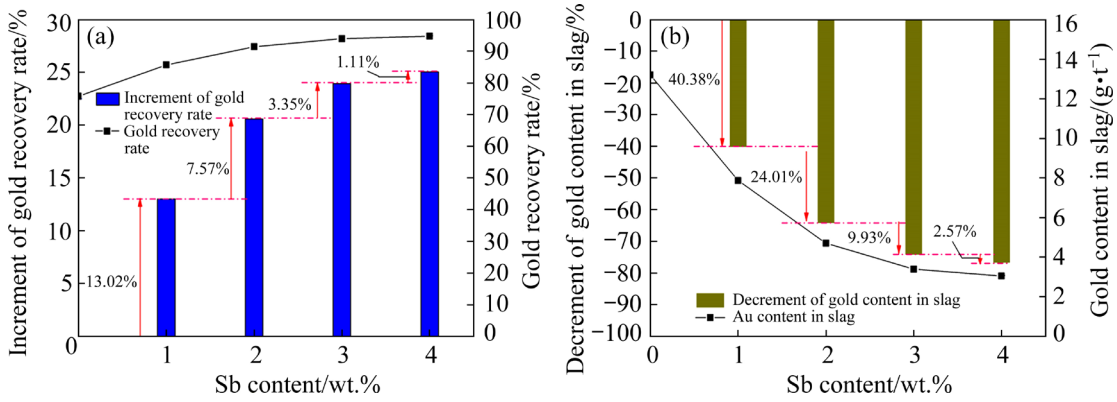

Fig. 6 Effect of Sb content on gold recovery rate (a) and gold content in slag (b)

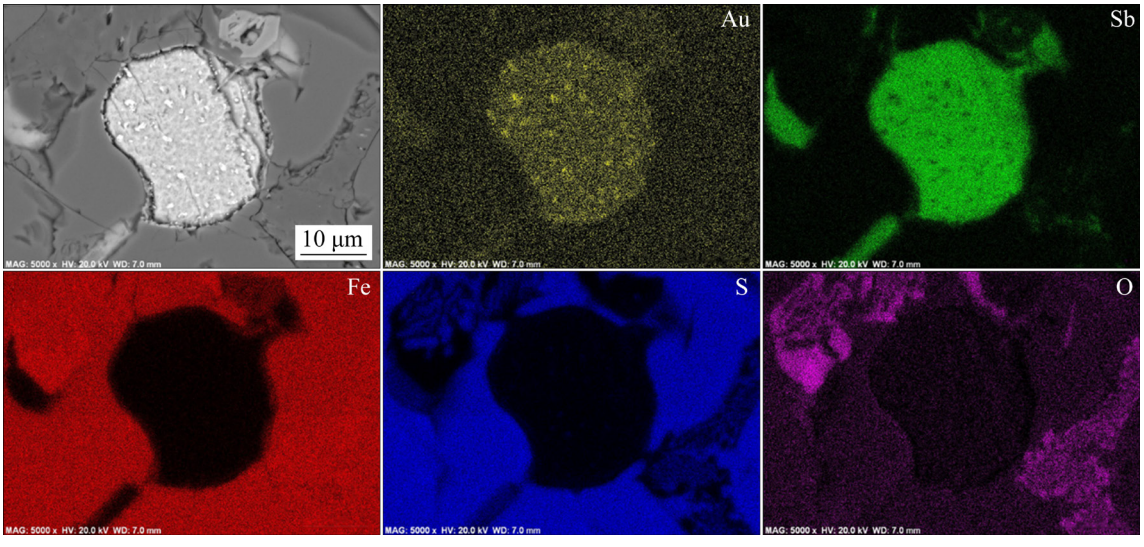

Fig. 7 Elemental surface scanning images of iron matte from experiments with addition of 4 wt.% Sb

3.2.2 Effect of As content

The effect of the As content in the raw materials on the gold recovery rate and gold content in slag was investigated. The As content was controlled by adding arsenic sulfide. The experimental conditions were maintained as follows: m(FeO)/m(SiO_2)=1.2, m(CaO)/m(SiO_2)=0.4, temperature of 1200 °C, and duration time of 45 min. The results are shown in Fig. 8.

As shown in Fig. 8, the gold recovery rate increased as the As content increased, whereas the gold content in the slag correspondingly decreased. When the As content increased from 0 to 6 wt.%, the gold recovery rate increased from 75.81% to 83.92%, representing a proportional increase of 10.70%. Meanwhile, the gold content in the slag decreased from 13.20 to 8.60 g/t, with a proportional decrease of 34.85%. Compared to Sb, the effect of As on the gold enhancement capture process was limited.

However, when the As content increased from 6 wt.% to 8 wt.%, the gold recovery rate decreased from 83.92% to 83.10%, whereas the gold content in the slag increased from 8.60 to 8.81 g/t. It is believed that when the As content in the raw material was too high, the proportion of As distributed in the slag increased, which may have indirectly affected the gold distribution. Therefore, the optimal As content was determined to be 6 wt.%.

Elemental surface scanning images of the iron matte for the experiments with 6 wt.% As addition are presented in Fig. 9. Multiple elemental gold particles were embedded within the As−Fe alloy, particularly at the interface with the iron matte. This result was consistent with that discussed in Section 3.1.2, which indicated that the As−Fe alloy captured free gold, leading to an increase in the particle size of the gold-loaded As−Fe alloy.

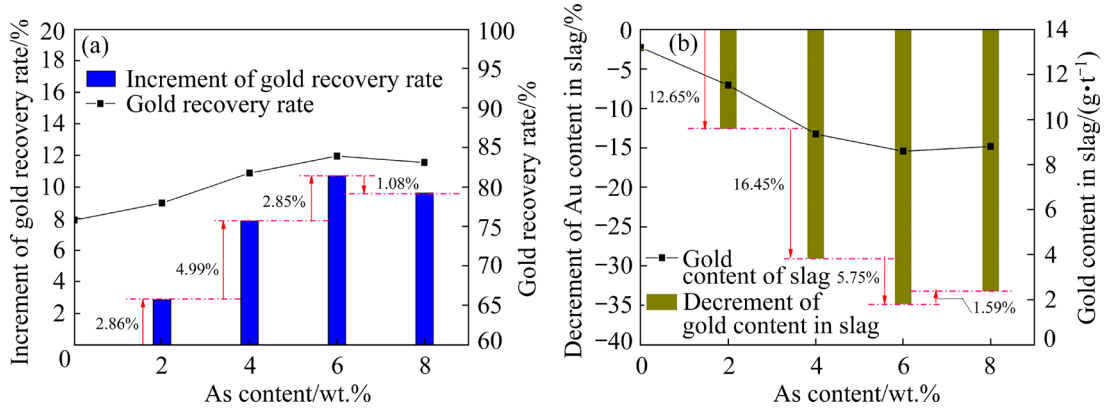

Fig. 8 Effect of As content on gold recovery rate (a) and gold content in slag (b)

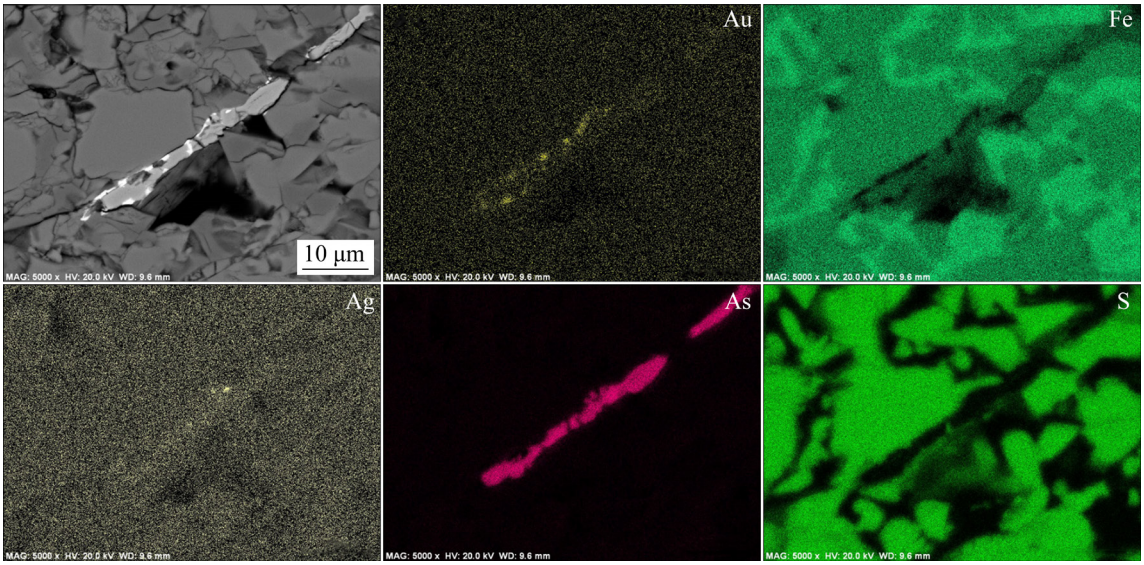

Fig. 9 Elemental surface scanning images of iron matte from experiments with addition of 6 wt.% As

3.2.3 Synergistic effect of Sb and As

As discussed in Sections 3.1 and 3.2, the gold recovery rates for the samples with 4 wt.% Sb and 6 wt.% As additions were lower than that of the As- and Sb-bearing refractory gold concentrate. This indicates that the effects of Sb and As on gold enhancement capture could be additive. The synergistic effects of Sb and As were subsequently explored, as described in the following section.

The Sb-removed gold concentrate (5.74 wt.% As) was used as the raw material, and antimony sulfide was added to modify the Sb content in the raw materials. The experimental conditions were controlled as follows: $m(FeO)/m(SiO_2)$=1.2, $m(CaO)/m(SiO_2)$=0.4, temperature of 1200 °C, and duration time of 45 min. The effects of Sb content (1 wt.%, 2 wt.%, 3 wt.%, and 4 wt.%) on the gold recovery rate and gold content in slag were studied. The results are presented in Fig. 10.

As shown in Fig. 10, Sb had a significant positive effect on gold capture. When the Sb content increased from 0 to 4 wt.%, the gold recovery rate increased from 85.67% to 97.12%, whereas the gold content in the slag decreased to 1.70 g/t. Compared to the results presented in Section 3.1, it is evident that the gold recovery rate is further improved with the help of As. Thus, the synergistic effect of Sb and As was confirmed.

The elemental surface scanning images of iron matte in the synergistic experiment are shown in Fig. 11. Sb existed in the form of the metal in iron matte, whereas gold existed as the Au−Sb alloy inside Sb. The combination tendency of Sb and Au was evident.

3.3 Optimal experimental product mineralogy

According to the previous study, the addition of Sb and As was confirmed to be 4 wt.% and 6 wt.%, respectively. Under the optimized conditions, the gold recovery rate reached 97.12%, and the gold content in the slag decreased to 1.70 g/t.

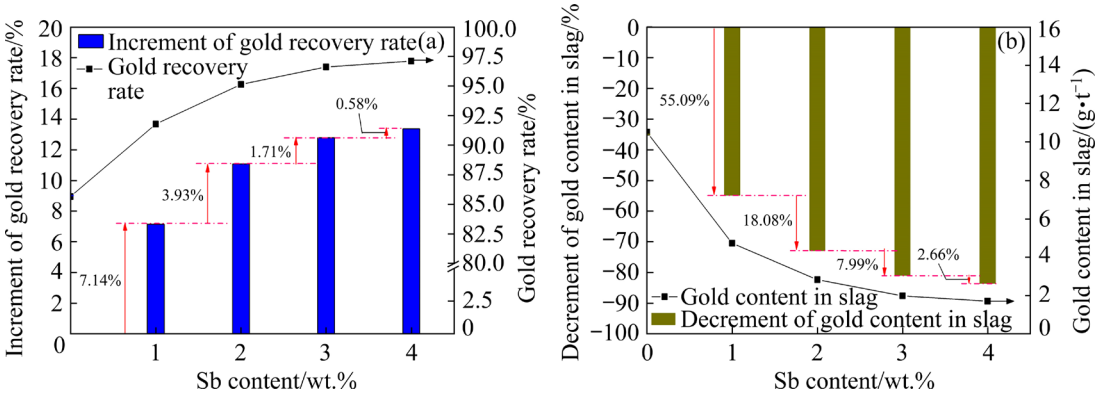

Fig. 10 Effect of Sb content on gold recovery rate (a) and gold content in slag (b) during synergistic effect experiment

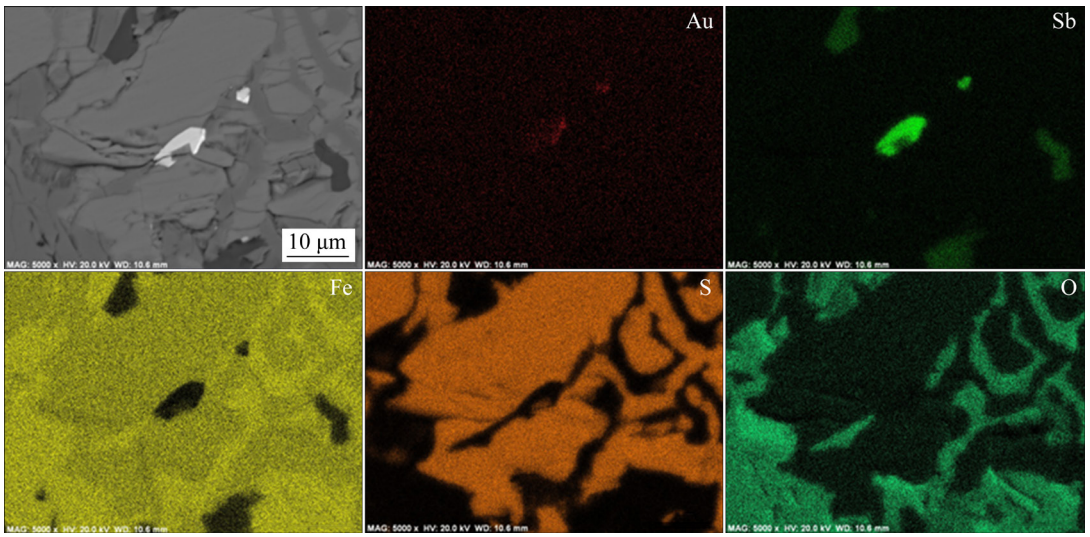

Fig. 11 Elemental surface scanning images of iron matte in synergistic experiment

The Sb content in the slag was only 0.52%, with a distribution rate of 8%. In contrast, the Sb content in the iron matte was 3.20 wt.%, and its distribution rate was 40%. Additionally, 52% of the Sb was distributed in the gas phase. This phenomenon can be attributed to the characteristics of Sb, which include a low melting point, the tendency to oxidize easily, and the propensity to volatilize. The occurrence state of Sb in the dust was Sb_2O_3.

The SEM image of the slag phase and chemical compositions of the typical phases from optimized experiment are shown in Fig. 12 and Table 5, respectively. There were only two phases in the slag: Point 1 represented the Sb−Fe alloy resulting from mechanical inclusion, whereas Point 2 represented the common phase of the slag.

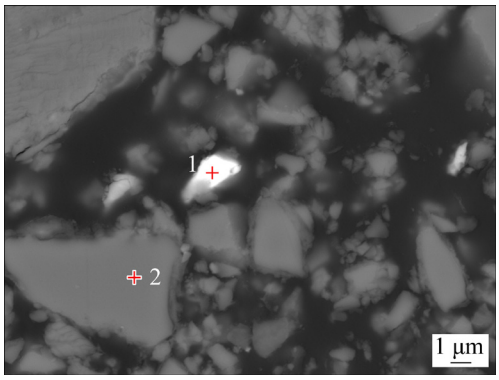

Fig. 12 SEM image of slag phase from optimized experiment

Table 5 Chemical compositions of typical phases in slag phase from optimized experiment (wt.%)

Point in Fig. 12	Sb	Fe	O	Si	Al	Ca	Others
1	79.76	17.83	1.67	0.74	−	−	−
2	−	18.00	34.13	25.96	5.04	13.96	2.91

The gold-loaded iron matte was analyzed using SEM, and the chemical compositions of different phases were determined using EDS. The results are presented in Fig. 13 and Table 6, respectively. A significant amount of Au−Sb alloy (Point 2) was observed to diffuse into the metallic Sb (Point 1). This indicates that Sb could effectively capture gold. The Au−Sb alloy was identified as $AuSb_2$, which agrees with the literature [30]. Furthermore, a comparison with Fig. 5 revealed that the size of the metallic Sb was larger than that of free gold.

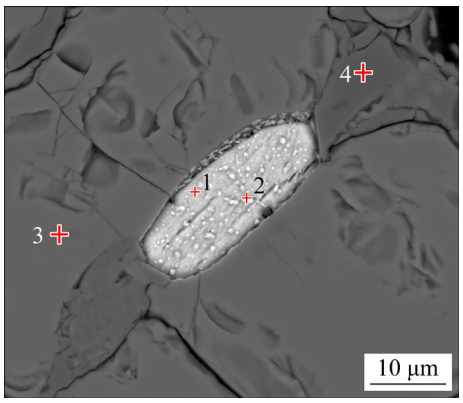

Fig. 13 SEM image of iron matte from optimized experiment

Table 6 Chemical compositions of typical phases in iron matte from optimized experiment (wt.%)

Point in Fig. 13	Au	Sb	Fe	S	O	Others
1	−	100	−	−	−	−
2	51.90	48.10	−	−	−	−
3	−	−	69.45	29.87	−	0.68
4	−	−	71.66	20.39	7.69	0.26

3.4 Comparison and summary

The impacts of Sb and As on gold enhancement capture by the iron matte are illustrated in Table 7. The enhancement effect of Sb was more pronounced than that of As, with optimal results achieved through the synergistic effect of both elements. A correlation between the gold recovery rate and the contents of Sb and As was established. The gold recovery rate could be effectively controlled by the quantitative addition of Sb and As, whether these elements were associated with the mineral or added later. This study demonstrated that the effects of Sb and As on gold enhancement capture are universal and controllable.

The mechanism of the gold enhancement capture process was concluded as follows. Owing to the strong alloying tendency between Au and Sb, a significant amount of free gold was captured and aggregated by Sb during the iron matte smelting process. In addition, the As−Fe alloy could capture free gold. The particle sizes of the gold-captured phases, including Au−Sb and As−Fe alloys, increased noticeably, resulting in a corresponding increase in settlement velocity. Consequently, the gold recovery rate increased significantly. The enhancement process is illustrated in the schematic diagram in Fig. 14.

Table 7 Sum of results of smelting using different raw materials

Raw material	Sb content/wt.%	As content/wt.%	Gold content in slag/(g·t^{-1})	Gold recovery rate/%	Occurrence state of gold
As- and Sb-bearing gold concentrate	4.05	6.17	2.05	96.44	Au−Sb alloy
Sb-removed gold concentrate	0.02	5.74	10.85	85.67	Metallic Au
As-removed gold concentrate	0.02	0.18	13.20	75.81	Au−Ag alloy
Sb-addition gold concentrate	4.00	0.18	3.05	94.80	Au−Sb alloy
As-addition gold concentrate	0.02	6.00	8.60	83.92	Metallic Au
Sb- and As-addition gold concentrate	4.00	5.74	1.70	97.12	Au−Sb alloy

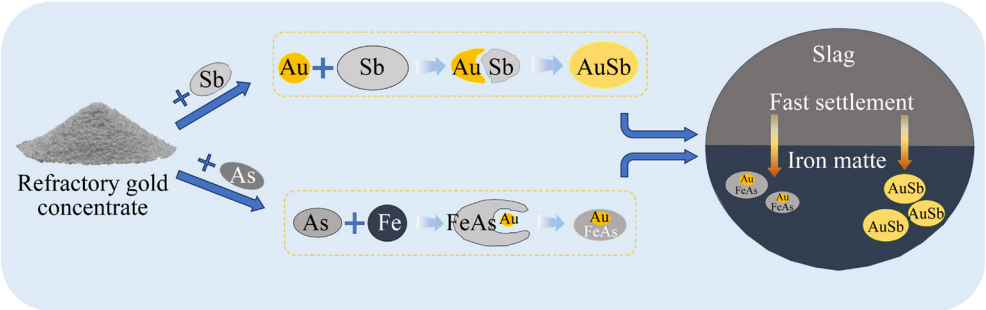

Fig. 14 Schematic diagram of gold enhancement capture process

4 Conclusions

(1) The exclusion method was employed to qualitatively study the effects of Sb and As on gold capture during iron matte smelting. Both Sb and As enhanced the gold capture process and influenced the gold occurrence state as well as the embedding relationships between typical mineral phases in the iron matte.

(2) The effects of the Sb and As contents on gold enhancement capture were investigated quantitatively. As the Sb and As contents increased, the gold recovery rate also increased. When the Sb content reached 4 wt.%, the gold recovery rate increased significantly to 94.80%. At the optimal As content of 6 wt.%, the gold recovery rate increased to 83.92%. The highest gold recovery rate (97.12%) was obtained with the synergistic effect of Sb and As. The enhancement effect of Sb and As was universal and controllable.

(3) The mechanism of gold enhancement capture was illustrated. Sb captured free gold and aggregated it within metallic Sb. The As−Fe alloy also captured free gold. The larger-sized gold-loaded phases showed faster settling velocities than free gold. Hence, the gold capture was enhanced.

CRediT authorship contribution statement

Bai-qi SUN: Experiments operation, Formal analysis, Visualization, Software, Investigation, Writing − Original draft; **Wei-feng LIU:** Conceptualization, Methodology, Validation, Writing − Review & editing; **Du-chao ZHANG:** Resources, Supervision, Data curation; **Lin CHEN:** Resources, Data curation; **Xu-heng LIU** and **Tian-zu YANG:** Writing − Review & editing.

Declaration of competing interest

The authors declare that they have no known competing financial interests or personal relationships that could have appeared to influence the work reported in this paper.

Acknowledgments

This work was financially supported from the National Natural Science Foundation of China (No. 52274358), the Natural Science Foundation of Hunan Province, China (No. 2020JJ4718), the Major Science and Technology Projects of Gansu Province, China (No. 22ZD6GC017), the Young Scientists Fund of National Natural Science Foundation of China (No. 51404296), and the National Key Research and Development Program of China (No. 2018YFC1901604).

References

[1] VAUGHAN J P. The process mineralogy of gold: The

classification of ore types [J]. JOM, 2004, 56: 46−48.

[2] PALENIK C S, UTSUNOMIYA S, REICH M, KESLER S E, WANG Lu-min, EWING R C. “Invisible” gold revealed: Direct imaging of gold nanoparticles in a Carlin-type deposit [J]. American Mineralogist, 2004, 89: 1359−1366.

[3] KYLE J H, BREUER P L, BUNNEY K G, PLEYSIER R. Review of trace toxic elements (Pb, Cd, Hg, As, Sb, Bi, Se, Te) and their deportment in gold processing [J]. Hydrometallurgy, 2012, 111/112: 10−21.

[4] JIN Shi-bin, MA Jin-rui, XING Zhi-jun, QIN Xiao-peng, YANG Bao-cheng. Influence of antimony on refractory gold ore roasting and cyaniding leaching [J]. Gold, 2009, 30(2): 33−37. (in Chinese)

[5] BARON J Y, CHOI Y, JEFFREY M. Double-refractory carbonaceous sulfidic gold ores [J]. Gold Ore Processing, 2016: 909−918.

[6] XU Rui, LI Qian, MENG Fei-yu, YANG Yong-bin, XU Bin, YIN Hua-qun, JIANG Tao. Bio-oxidation of a double refractory gold ore and investigation of preg-robbing of gold from thiourea solution [J]. Metals, 2020, 10(9): 1216.

[7] HAPID A, ZULLAIKAH S, MAHFUD A, KAWIGRAHA A, SUDIYANTO Y, NARESWARI R B, QUITAIN A T. Oxidation of sulfide mineral and metal extraction analysis in the microwave-assisted roasting pretreatment of refractory gold ore [J]. Arabian Journal of Chemistry, 2024, 17: 105447.

[8] QIN Hong, GUO Xue-yi, TIAN Qing-hua, YU Da-wei, ZHANG Lei. Recovery of gold from sulfide refractory gold ore: Oxidation roasting pretreatment and gold extraction [J]. Minerals Engineering, 2021, 164: 106822.

[9] KANG Jian, YAO Ze-yu, HU Liang-xun, WANG An, HUANG Peng, LIU Shuang, ZHU Dan. Experimental study on alkaline pressure pre-oxidation−cyanide leaching of low-grade carbonaceous gold ore in Hubei Province [J]. Gold, 2024, 45(6): 37−40. (in Chinese)

[10] GUI Qi-hao, FU Li-kang, HU Yu-ting, DI Hao-kai, LIANG Ming, WANG Shi-xing, ZHANG Li-bo, DONG En-hua. Oxidative pretreatment of refractory gold ore using persulfate under ultrasound for efficient leaching of gold by a novel eco-friendly lixiviant: Demonstration of the effect of particle size and economic benefits [J]. Hydrometallurgy, 2023, 221: 106110.

[11] HONG Mao-xin, WANG Jun, YANG Bao-jun, LIU Yang, LIAO Rui, YU Shi-chao, LIU Shi-tong, TANG An-ni, WANG Wei, QIU Guan-zhou. Bio-dissolution and kinetics of pyrite-bearing waste ores in presence of *Acidithiobacillus ferrooxidans* [J]. Transactions of Nonferrous Metals Society of China, 2024, 34: 2342−2353.

[12] BAS A D, GAVRIL L, ZHANG W, GHALI E, CHOI Y. Electrochemical dissolution of roasted gold ore in cyanide solutions [J]. Hydrometallurgy, 2015, 156:188−198.

[13] MSUMANGE D A, YAZICI E Y, CELEP O, DEVECI H, KRITSKII A, KARIMOV K. Recovery of Au and Ag from the roasted calcine of a copper-rich pyritic refractory gold ore using ion exchange resins [J]. Minerals Engineering, 2023, 195: 108017.

[14] LI Ke, LI Qian, JIANG Tao, YANG Yong-bin, XU Bin, XU Rui, ZHANG Yan. Thiourea leaching of gold in presence of jarosite and role of oxalate [J]. Transactions of Nonferrous Metals Society of China, 2024, 34: 322−335.

[15] LI Qian, ZHU Yue-hong, ZHANG Yan, MA Yong-he, YANG Yong-bin. Research progress and prospect of non-cyanide gold lixiviants [J]. The Chinese Journal of Nonferrous Metals, 2024, 34: 2356−2382. (in Chinese)

[16] OU Yang, YANG Yong-bin, WANG Lin, LI Ke, GAO Wei, ZHANG Yan, LI Qian, JIANG Tao. A clean and efficient innovative technology for refractory sulfide gold ore: In situ gold extraction via self-generated thiosulfate [J]. Journal of Cleaner Production, 2023, 419: 138280.

[17] KANG Jin-xing, YU Chen, WANG Xin, LIU Zhi-guo, WANG Ya-yun. A novel non-cyanide extraction method of gold for high As−Sb-bearing refractory gold ore based on Mn-oxide ore acidic oxidation [J]. Chemical Engineering Research and Design, 2022, 189: 347−357.

[18] WANG J X, FARAJI F, RAMSAY J, GHAHREMAN A. A review of biocyanidation as a sustainable route for gold recovery from primary and secondary low-grade resources [J]. Journal of Cleaner Production, 2021, 296: 126457.

[19] SHIN D, JEONG J, LEE S, PANDEY B D, LEE J C. Evaluation of bioleaching factors on gold recovery from ore by cyanide-producing bacteria [J]. Minerals Engineering, 2013, 48: 20−24.

[20] KONADU K T, MAKAULA D X, SMART M, CINDY, MENDOZA D M, OPITZ E, HARRISON S T L, SASAKI K. Enzymatic degradation of carbonaceous matter in contrasting South African refractory gold ores using cell-free spent medium from Phanerochaete chrysosporium [J]. Hydrometallurgy, 2023, 220: 106087.

[21] AVARMAA K, JOHTO H, TASKINEN P. Distribution of precious metals (Ag, Au, Pd, Pt, and Rh) between copper matte and iron silicate slag [J]. Metallurgical and Materials Transactions B, 2016, 47: 244−255.

[22] CHEKUSHIN V S, OLEINIKOVA N V, TYCHENKO A I. The extraction of gold from sulfide concentrates into molten lead [J]. Russian Journal of Non-ferrous Metals, 2008, 49: 340−345.

[23] WANG Qin-meng, WANG Song-song, TIAN Miao, TANG Ding-xuan, TIAN Qing-hua, GUO Xue-yi. Relationship between copper content of slag and matte in the SKS copper smelting process [J]. International Journal of Minerals, Metallurgy, and Materials, 2019, 26: 301−308.

[24] GUO Xue-yi, WANG Song-song, WANG Qin-meng, TIAN Qing-hua, WANG Zhi, WANG Yong-jun, PENG Guo-min, ZHAO Bao-jun. Mechanism of gold collection in matte and distribution behavior of precious metals in oxygen-enriched smelting process [J]. Transactions of Nonferrous Metals Society of China, 2020, 30: 2951−2962.

[25] SHISHIN D, HIDAYAT T, SULTANA U, SHEVCHENKO M, JAK E. Experimental study and thermodynamic calculations of the distribution of Ag, Au, Bi, and Zn between Pb metal and Pb−Fe−O−Si slag [J]. Journal of Sustainable Metallurgy, 2020, 6: 68−77.

[26] YANG Tian-zu, LU Yi-fan, ZHANG Du-chao, LIU Wei-feng, CHEN Lin, LING Hong-bin. Enriching gold from refractory arsenic-bearing gold ore by matte smelting method [J]. Precious Metals, 2019, 40: 5−11. (in Chinese)

[27] YANG Tian-zu, XIE Bo-yi, LIU Wei-feng, ZHANG Du-chao, CHEN Lin. Enrichment of gold in antimony matte by direct

smelting of refractory gold concentrate [J]. JOM, 2018, 70: 1017−1023.

[28] HIDAYAT T, CHEN J, HAYES P C, JAK E. Distributions of Ag, Bi, and Sb as minor elements between iron-silicate slag and copper in equilibrium with tridymite in the Cu−Fe−O−Si system at T=1250 °C and 1300 °C (1523 K and 1573 K) [J]. Metallurgical and Materials Transactions B, 2018, 50: 229−241.

[29] GE Yang, LIU Zhi-hong, YU Zhi-qian, WANG Huan-wen, LU Xing-wu, ZHANG Le-ru, XIA Long-gong. Distribution behaviors of As, Sb, Bi, Sn, Se, Te, Au and Ag between Cu and liquid metal phases in the Cu−Pb binary system at 500−1080 °C [J]. JOM, 2023, 75: 1515−1529.

[30] OKAMOTO H, SCHLESINGER M E, MUELLER E M. ASM handbook: Alloy phase diagrams (Vol. 3) [M]. 2nd ed. New York: ASM International, 2016.

排除法研究锑和砷对难处理金矿造铁锍熔炼过程中金强化捕集的影响

孙百奇[1]，刘伟锋[1,2]，张杜超[1,2]，陈 霖[1,2]，刘旭恒[1,2]，杨天足[1]

1. 中南大学 冶金与环境学院，长沙 410083；
2. 中南大学 低碳有色冶金国家工程研究中心，长沙 410083

摘 要：基于锑(Sb)和砷(As)的性质特点，提出了一种利用 Sb 和 As 提高造铁锍熔炼过程中金回收效果的方法，并利用排除法研究了 Sb 和 As 对强化捕金效果的影响。结果表明，Sb 和 As 能显著提高金回收率，且金回收率随 Sb 或 As 含量的增加而增加。Sb 的强化效果优于 As，且在 Sb 和 As 协同作用下能得到最优强化效果：金回收率达到 97.12%，而渣中金含量降低至 1.70 g/t。Sb 能捕集和汇聚游离金，并形成 Au−Sb 合金。As−Fe 合金同样能捕集游离金。捕金物相粒度增大使其沉降速度增加，从而促进金的回收。

关键词：难处理金矿；Au−Sb 合金；As−Fe 合金；强化作用；铁锍；捕金

(Edited by Wei-ping CHEN)